CDDpress

www.nature.com/cddiscovery

ARTICLE OPEN

The chemical chaperone 4-phenylbutyric acid rescues molecular cell defects of *COL3A1* mutations that cause vascular Ehlers Danlos Syndrome

Ramla Omar[1], Michelle AW Lee[1], Laura Gonzalez-Trueba[1], Cameron R. Thomson[1], Uwe Hansen[2], Spyridonas Lianos[1], Snoopy Hazarika[1], Omar El El Abdallah[1], Malak A. Ammar[1], Jennifer Cassels[3], Alison M. Michie[3], Neil J. Bulleid[4], Fransiska Malfait[5] and Tom Van Agtmael[1]✉

Vascular Ehlers Danlos Syndrome (vEDS) is a connective tissue disorder caused by *COL3A1* mutations for which there are no treatments due to a limited understanding of underlying mechanisms. We aimed to identify the molecular insults of mutations, focusing on collagen folding, to establish if targeting protein folding represents a potential therapeutic approach. Analysis of two novel *COL3A1* glycine mutations, G189S and G906R, in primary patient fibroblast cultures revealed secretion of misfolded collagen III and intracellular collagen retention leading to lower extracellular collagen levels. This was associated with matrix defects, endoplasmic reticulum (ER) stress, reduced cell proliferation and apoptosis. The ER stress was mediated by activation of IRE1 and PERK signalling arms with evidence of allelic heterogeneity. To establish if promoting ER protein folding capacity or protein degradation represents novel therapeutic avenues, we investigated the efficacy of FDA-approved small molecules. The chemical chaperone 4-phenylbutyric acid (PBA) rescued the ER stress and thermostability of secreted collagen leading to reduced apoptosis and matrix defects, and its efficacy was influenced by duration, dosage and allelic heterogeneity. Targeting protein degradation with carbamazepine (CBZ), or PBA-CBZ in combination did not increase treatment efficacy. These data establish that ER stress is a molecular mechanism in vEDS that can be influenced by the position of *COL3A1* mutation. It combines with matrix defects due to reduced collagen III levels and/or mutant protein secretion to vEDS pathogenesis. Targeting protein folding using FDA-approved chemical chaperones represents a putative mechanism-based therapeutic approach for vEDS that can rescue intra- and extracellular defects.

Cell Death Discovery (2025)11:200 ; https://doi.org/10.1038/s41420-025-02476-y

INTRODUCTION

Vascular Ehlers Danlos Syndrome (vEDS) (OMIM # 130050) is a rare heritable connective tissue disorder caused by heterozygous mutations in the gene *COL3A1* that encodes the alpha 1 chain of collagen III, α1(III) [1]. VEDS is a multi-systemic disorder that significantly reduces life expectancy mostly due to dissection and rupture of arteries, intestine and gravid uterus [2]. Other features include translucent, thin skin that tears and bruises easily and has delayed wound healing, early-onset varicose veins, small joint hypermobility, tendon- and muscle ruptures, pneumo(hemo) thorax, carotid-cavernous fistula, and characteristic facial features [3].

Collagen III is a major fibrillar collagen in the extracellular matrix (ECM) that is highly expressed in soft tissues with elastic properties including dermis, blood vessels, and gastro-intestinal tract [4–6]. It is folded in the endoplasmic reticulum (ER) where three α1(III) chains interact to form a triple helical collagen III molecule in a zipper like fashion from C- to N-terminal end [7, 8]. The triple helical collagenous domain is composed of Gly-Xaa-Yaa repeats with every third amino acid being a glycine, and ~66% of *COL3A1* mutations affect glycines [9, 10]. Mutations in other collagens reduce extracellular collagen levels and induce ER stress with activation of the unfolded protein response (UPR) that can be targeted by FDA- and EMA-approved small compounds [11–17]. Although the first *COL3A1* mutations were identified ~40 years ago major gaps in our understanding of their molecular mechanism remain [1]. In particular, while ECM defects are a defining feature the impact of glycine substitutions, which account for 95% of mutations, on protein folding remains unclear.

This gap in our mechanistic knowledge is hindering the development of mechanism-based treatments. The only treatment for vEDS, in Europe, is the beta blocker celiprolol and whilst it has some efficacy [18], it is not well tolerated (1/3 patients do not tolerate recommended dose) [19] and was declined FDA

[1]School of Cardiovascular and Metabolic Health, College of Medical, Veterinary & Life Sciences, University of Glasgow, Glasgow G12 8QQ, UK. [2]Institute of Musculoskeletal Medicine, University of Muenster, University Hospital Muenster, D-48149 Muenster, Germany. [3]Paul O'Gorman Leukaemia Research Centre, School of Cancer Studies, College of Medical, Veterinary & Life Sciences, University of Glasgow, Glasgow, UK. [4]School of Molecular Biosciences, College of Medical, Veterinary & Life Sciences, University of Glasgow, Glasgow G12 8QQ, UK. [5]Center for Medical Genetics, Ghent University Hospital and Department for Biomolecular Medicine, Ghent University, Corneel Heymanslaan 10, 9000 Ghent, Belgium. Posthumous authorship:Neil J. Bulleid. See author contributions. ✉email: tom.vanagtmael@glasgow.ac.uk

Received: 2 July 2024 Revised: 14 February 2025 Accepted: 4 April 2025
Published online: 25 April 2025

Table 1. Clinical and demographic information of patients.

	Patient 1	Patient 2
Mutation	COL3A1 G189S	COL3A1 G906R
Demographic	Caucasian, Male	Caucasian, female
Age at diagnosis and skin biopsy collection	36	37
Arterial Phenotype	Dissection aorta Iliaca right, aneurysm renal aorta, aneurysm left aorta Iliaca. Vena porta rupture; all between age 30-36 yrs	Aneurysm in Right arteria subclavia (detected age 19), multiple aneurysms on MRI at age 37
Gastro-intestinal	No gastro-intestinal complications	No gastro-intestinal complications
Skin phenotype	Normal skin but easy bruising	Thin skin with easy bruising
Other phenotypes	Hypermobility of small joints	No uterine complications
		Deceased aged 50 post aortic dissection

approval. Experimental treatments have focused on targeting more downstream pathways or modulating known risk factors that predispose to vascular rupture such as blood pressure [1, 20–22]. Inhibiting PKC/MEK/ERK signalling (e.g. via cobimetinib), improved survival [20] in some but not all mouse models harbouring *Col3a1* mutations [21]. Considering the multi-systemic nature of the disease that affects different cell types, targeting single downstream pathways may only be effective for particular cell types and/or mutations, as found for celiprolol treatment in mice [20, 22]. This underscores the need for complementary approaches that directly target upstream molecular insults of the mutations.

Here, using primary patient fibroblasts we set out to address the impact of two novel *COL3A1* glycine mutations, *COL3A1*$^{+/G906R}$ and *COL3A1*$^{+/G189S}$, on collagen folding and establish the efficacy of FDA-approved compounds that target protein folding or degradation on the cell phenotype. Our data show that glycine *COL3A1* mutations lead to secretion of mutant collagen III while also differentially activating the UPR. Importantly, the FDA-approved chemical chaperone 4-phenylbutyric acid (PBA) rescues both of these molecular insults and improves cell viability. We also interrogated dosage and duration as treatment parameters and establish that targeting protein folding using chemical chaperones represents a potential therapeutic strategy for vEDS.

RESULTS

COL3A1 glycine mutations have a quantitative and qualitative effect in vEDS

To explore pathomolecular mechanisms of *COL3A1* glycine mutations, we established primary dermal fibroblasts cultures of two vEDS patients. The clinical and demographic information is provided in Table 1. Both mutations affect glycine residues of the Gly-Xaa-Yaa repeat in α1(III) with the more N-terminal mutation in exon 6 leading to a glycine to serine substitution (G189S), and the more C-terminal mutation altering glycine to arginine in exon 31 (G906R) (Fig. 1A-B). The G189S mutation is absent in gnomAD and ClinVar, but G189R (rs587779507) has been reported on dbSNP and ClinVar. Analysis using Variant Effect Predictor software in Ensembl (SIFT, PolyPhen, CADD score) classified both variants as deleterious (Table 2), supporting the causality of these two mutations.

Both mutations caused a reduction in cell proliferation (Fig. 1C, Supplemental Fig. 1A) with increased apoptosis (Fig. 1D, Supplemental Fig. 1B) and we also observed altered morphology of mutant cells which was particularly pronounced in *COL3A1*$^{+/G189S}$ cells, looking flatter with an irregular larger "pancake" type morphology compared with wild type (WT) fibroblasts (Fig. 1E), a key morphological feature of senescent cells [23]. These features coupled with increased levels of the senescence marker p21 in *COL3A1*$^{+/G189S}$ (Fig. 1F) [24], suggest senescence induction due to *COL3A1* mutations.

Non-mutually exclusive impacts of collagen mutations include secretion of mutant protein, reduced extracellular protein levels and/or protein misfolding leading to ER stress [1, 25]. To shed light on these, we determined if these mutations affect collagen III secretion. This revealed increased intracellular collagen III levels in both mutant cells with reduced (G189S) or similar (G906R) extracellular levels (Fig. 2A-B), indicating a shift towards intracellular retention. Immunostaining against collagen III and the ER marker PDI confirmed collagen III was retained in the ER (co-localisation coefficient value (Pearson's R): WT: 0.668, COL3A1 G189S 0.721, COL3A1 G906R: 0.815) and also supported ER enlargement (Fig. 2C), a sign of ER stress, which was corroborated by EM analysis of the cells (Supplemental Fig. 2).

While *COL3A1* nonsense mutations show reduced protein levels can be pathogenic, the increased severity of glycine substitutions supports a dominant negative effect [3, 9], potentially by secreting mutant protein. Missense mutations in collagens can affect their thermostability due to the impact on triple helix formation and their folding. We used sensitivity to trypsin digestion as a proxy of the folding quality of triple helical secreted collagen III. This revealed that secreted collagen III from mutant cells is digested more rapidly (Fig. 2D) and that both glycine mutations enable secretion of misfolded collagen III. This is associated with an altered more punctate appearance of the deposited collagen III network with apparently less fibrils (Fig. 2E). These data show that collagen III mutations act via quantitative and qualitative effects by reducing levels of extracellular collagen III coupled with secreting mutant less stable collagen III.

vEDS mutations activate the unfolded protein response

Misfolding of secreted proteins can lead to ER stress and activation of the UPR, which consists of three signalling arms mediated by PERK, IRE1 and ATF6 [26]. IRE1 activation leads to "splicing" of the mRNA XBP1, while PERK phosphorylates eIF2α and causes upregulation in mRNA translation of ATF4 [26]. *COL3A1* mutant cells had increased levels of the ER chaperone BIP (Fig. 3A-B) with a more prominent activation of the IRE1 arm, in particular in *COL3A1*$^{+/G906R}$ (Fig. 3C). Similarly, while both mutations caused EIF2α phosphorylation, only *COL3A1*$^{+/G906R}$ showed increased levels of ATF4, although a trend was observed in *COL3A1*$^{+/G189S}$ cells (Fig. 3A-B). We did not detect activation of the ATF6 arm (Fig. 3A-B), indicating *COL3A1* mutations do not activate all arms of the classical ER stress response. The increased levels of CHOP (Fig. 3D) in *COL3A1*$^{+/G906R}$ cells but not *COL3A1*$^{+/G189S}$ support presence of ER stress-associated apoptosis. ER stress can activate protein degradation pathways to decrease misfolded protein levels in the ER [26]. Western blotting revealed activation of proteasomal degradation pathways, shown by increased levels of poly-ubiquitinated proteins, but not of autophagy, probed by assessing LC3I to LC3II conversion (Fig. 3E). Western blotting against p62 in absence or presence of bafilomycin A1 revealed no difference in autophagy flux (Supplemental Fig. 1C).

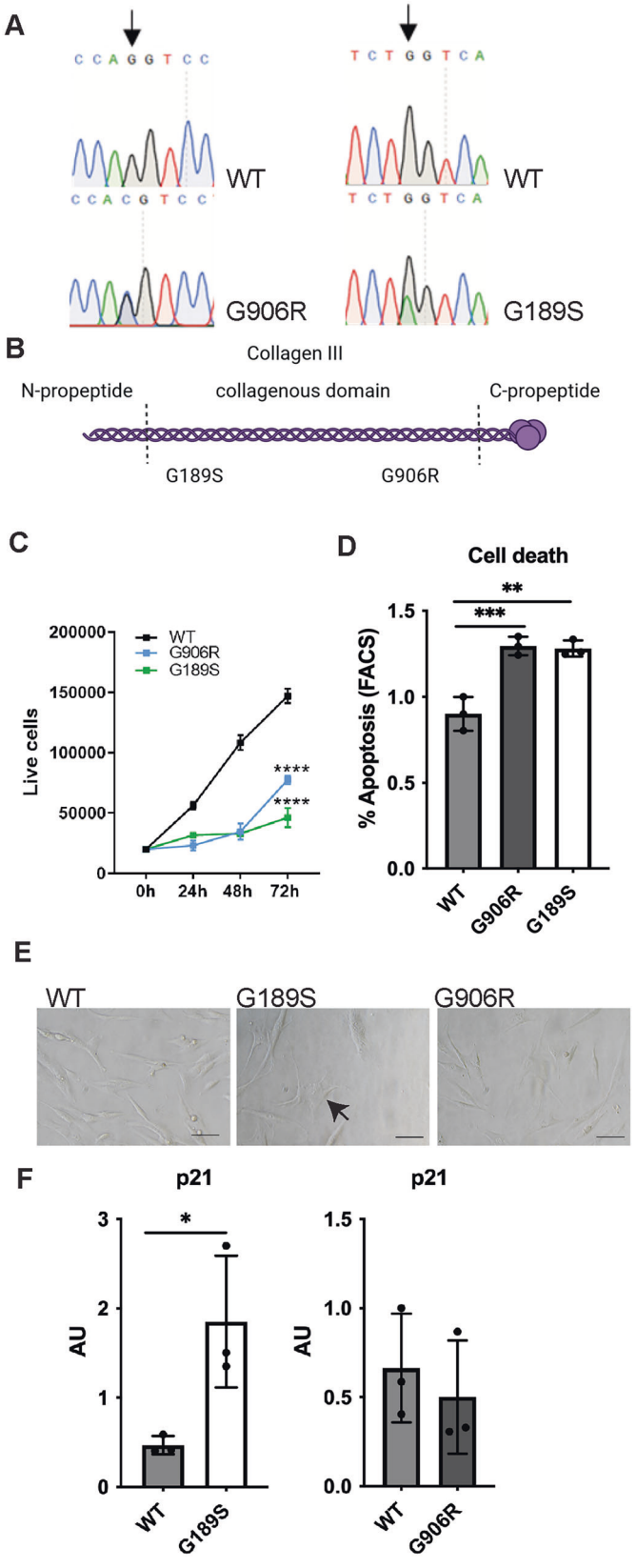

Fig. 1 Identification and functional defects of *COL3A1* mutations. (**A**) Sanger sequence traces of PCR products from DNA of primary patient fibroblasts cultures, covering *COL3A1* G906R and G189S mutation. WT: control primary dermal fibroblast. Black arrow indicates position of heterozygous mutation. (**B**) Diagram showing position of mutation within the collagen III protein and protein domain structure. (**C**) Cell proliferation analysis of wild type (WT), $COL3A1^{G189S/+}$ (G189S) and $COL3A1^{G906/+}$ (G906R) cells (n = 3, Two-Way ANOVA). (**D**) Percentage apoptotic cells determined by FACS (Annexin V, propidium iodide positive, FACS scatter plot provided in Supplemental Fig. 1)) of wild type (WT), $COL3A1^{G189S/+}$ (G189S) and $COL3A1^{G906/+}$ (G906R) cells (n = 3; One-way ANOVA with Dunnett's multiple comparison test). (**E**) Brightfield microscopy shows flattened irregular shaped enlarged cells particularly in $COL3A1^{G189S/+}$. (**F**) qRT-PCR reveals increased mRNA levels of p21, marker of senescence, in $COL3A1^{G189S/+}$ cells (n = 3, Mann-Whitney test). * $p < 0.05$; ** $p < 0.01$; *** $p < 0.001$ **** $p < 0.0001$.

These data establish that *COL3A1* mutations induce differential UPR activation with a more extensive and chronic ER stress due to the C-terminal $COL3A1^{+/G906R}$ mutation.

Targeting protein folding using PBA rescues intracellular phenotypes

Conceptually, pharmacologically targeting collagen folding and/or mutant protein degradation could modulate both the ER stress and ECM defects by promoting collagen secretion [15, 16, 27] and/or secretion of better-folded collagen. This could represent an avenue for rescuing both extra- and intracellular effects and be effective across different *COL3A1* mutations and tissues. This would overcome the genotype-dependent efficacy of recently proposed strategies that target more downstream mechanisms or blood pressure [20–22]. The availability of FDA-approved compounds, including PBA, TUDCA and CBZ, that target protein folding or degradation is particularly interesting as these are well-tolerated with good safety records [28], and repurposing FDA/EMA-approved compounds is an attractive cost-effective strategy for developing treatments for rare diseases [29].

We therefore set out to investigate their efficacy on *COL3A1* mutations by first incubating cells for 24 hours with different concentrations of PBA (1 mM, 5 mM, 10 mM), TUDCA (10 µM, 100 µM, 1 mM) and CBZ (10 µM, 20 µM, 1 mM) to assess the highest concentration that is tolerated by control primary dermal fibroblasts. Analysis revealed reduced viability with 10 mM PBA and 1 mM CBZ, while cell survival was not impacted by TUDCA treatment up to 1 mM (Supplemental Fig. 3).

As PBA can alleviate cellular defects due to mutations in other collagen types [15–17, 30], we first investigated its efficacy on vEDS fibroblasts. Incubating cells in 5 mM PBA for 24 hours reduced BIP protein levels in $COL3A1^{+/G189S}$ but not $COL3A1^{+/G906R}$ cells (Fig. 4A-B). To establish if the reduction in BIP levels is shared with other chemical chaperones we incubated vEDS cells with 500 µM TUDCA. This also reduced levels of BIP in $COL3A1^{+/G189S}$ cells (Supplemental Fig. 4), supporting that the reduction in BIP levels is at least in part due to effects on protein folding. In contrast, CBZ did not alter BIP protein levels or the phospho-Eif2α:total Eif2α ratio, revealing no ER stress reduction (Supplemental Fig. 5) through promotion of protein degradation, in contrast to what is achieved in *COL10A1* mutations [14]. These data show that chemical chaperones can rescue ER stress caused by *COL3A1* mutations but with allelic-specific effects as the C-terminal mutation was more resistant to treatment.

PBA dosage impacts treatment efficacy

Treatment dosage is an important consideration for any future treatments and given the allele specific effects, we set out to explore the impact of PBA dosage on its efficacy. Cells were incubated with four PBA concentrations for 24 hours and ER stress was measured. This revealed PBA reduces levels of BIP and the PERK pathway in $COL3A1^{+/G189S}$ across the different concentrations (Fig. 4C-D, Supplemental Fig. 5). In contrast only lower PBA

Table 2. In silico analysis of *COL3A1* mutations.

SYMBOL	EXON	cDNA	Protein	SIFT	PolyPhen	CADD_PHRED
COL3A1	6/51	682	G189S	deleterious(0.01)	probably_damaging(1)	32
COL3A1	39/51	2833	G906R	deleterious(0)	probably_damaging(0.999)	31

CADD > 20 and >30 indicate top 1% and top 0.1% of single nucleotide variants.

concentrations reduced ER stress marker levels in *COL3A1*$^{+/G906R}$ (Fig. 4C-D, Supplemental Figure 6).

We further characterised the effects of 24 hour incubation with 5 mM and 500 µM PBA on *COL3A1*$^{+/G189S}$ which revealed that 5 mM PBA significantly reduced spliced XBP1 levels with a trend towards lower CHOP mRNA levels in COL3A1$^{+/G189S}$ (Fig. 4E-H). This provides evidence for potential higher efficacy of 5 mM PBA compared to 500 µM. In contrast, 500 µM PBA, the concentration that showed most promising effect on BIP and EIF2α phosphorylation in *COL3A1*$^{+/G906R}$, had no effect on CHOP or spliced XBP1 levels (Fig. 4I-J). Given the absence of impact of higher dosage on BIP, we employed 500 µM PBA in *COL3A1*$^{+/G906R}$ cells.

To investigate if the lower ER stress levels were associated with reduced ER retention of collagen III, we performed western blotting on cell lysates. This supported reduced intracellular α1(III) retention in *COL3A1*$^{+/G189S}$ but not *COL3A1*$^{+/G906R}$ despite the modulated BIP levels and p-EIF2α/EIF2α ratio (Fig. 5A-B). Given the limited efficacy of 500 µM PBA in *COL3A1*$^{+/G906R}$, we next explored the impact of increased treatment duration for *COL3A1*$^{+/G906R}$. This revealed that a 72 hour incubation reduced intracellular collagen III levels (Fig. 5A-B), which was confirmed by immunostaining showing reduced ER retention of collagen III and ER area (co-localisation coefficient value (Pearson's R) between collagen III and PDI : COL3A1 G189S 0.668, COL3A1 G906R: 0.751; Fig. 5C-D). These data establish increased efficacy with a longer PBA incubation.

To explore why 72-hour and not 24-hour incubation with PBA reduced collagen III levels in *COL3A1*$^{+/G906R}$, we determined *COL3A1* mRNA levels as PBA can also have HDAC inhibitor activity [28]. This revealed genotype dependent effects with increased mRNA levels with 24 hour 500 µM PBA but not 72-hours for *COL3A1*$^{+/G906R}$, and reduced *COL3A1* mRNA levels in *COL3A1*$^{+/G189S}$ (Supplemental Fig. 4). This apparent pulse in expression could explain the lack of intracellular collagen III reduction with 24 hour PBA incubation in *COL3A1*$^{+/G906R}$ cells. We also explored if a combinatorial treatment that simultaneously targeted protein folding and degradation increased efficacy for *COL3A1*$^{+/G906R}$. Coupling 500 µM PBA with 20 µM CBZ for 24 hours did not reduce intracellular collagen III levels (Supplemental Figure 7A). Combined, these data support that PBA can rescue the ER stress due to *COL3A1* missense mutations and that dosage and treatment duration are important treatment parameters to help overcome allele dependent intracellular effects.

PBA rescues extracellular defects

We next set out to determine the impact of PBA on secreted collagen III given the established role of matrix defects in vEDS [1]. Western blotting of conditioned media indicated that PBA did not significantly increase the levels of collagen III secreted over a 24 hour period (Supplemental Figure 7B). However, the secreted collagen III was more resistant to trypsin digestion (Fig. 5F), and there was increased collagen III incorporation into the deposited ECM that showed a better-formed network (Fig. 5G). Furthermore, PBA treatment also reduced the apoptosis of patient fibroblasts (Fig. 5H). Therefore, PBA increased the quality of the secreted collagen and rescued both intracellular and extracellular sequelae as well as apoptosis due to *COL3A1* mutations.

DISCUSSION

Here, we provide novel insight into the molecular basis of genotype-phenotype correlation and mechanisms of vEDS by uncovering that glycine *COL3A1* mutations lead to secretion of mutant protein coupled with retention of collagen III in the ER that causes allele-specific UPR activation, apoptosis and ECM defects. Targeting protein folding using the FDA-approved chemical chaperone PBA rescues the ECM, molecular and cellular defects of these mutations and treatment duration is an important parameter to help overcome allele-specific effects of mutations. Combined these data support PBA represents a putative mechanism-based therapeutic approach for vEDS.

Glycine mutations account for the majority of *COL3A1* mutations in vEDS [9, 10] but their molecular mechanisms and that of vEDS remain poorly understood. Genetics data and outcomes in pre-clinical treatments [9, 20, 21] support allele-specific effects but the molecular basis of any genotype-phenotype correlation remains incomplete. Our data provide strong support that combined with secreting misfolded protein, *COL3A1* mutations can induce ER stress. They are also suggestive that a more extensive and chronic ER stress may occur due to the C-terminal *COL3A1*$^{+/G906R}$ mutation that include activation of the PERK and IRE1 signalling arms, which appeared more resistant to treatment. This raises a potential hypothesis that differential UPR activation may contribute to the basis of the genotype-phenotype correlation in vEDS. The suggested increased severity of the *COL3A1*$^{+/G906R}$ mutation could relate to the characteristics of the mutation as replacement of glycine with a larger amino acid is associated with more severe vEDS [9], and arginine in G906R is larger than serine in the more N-terminal *COL3A1 G189S* mutation. Moreover, it can reflect a positional effect as more C-terminal mutations have been associated with increased disease severity in fibrillar collagen disorders [31]. It is tempting to suggest this is due to more detrimental impact on protein folding with mutations closer to the initiation site of triple helix formation, which proceeds in a C- to N-terminal direction end [1, 7, 8]. If so, it may be that the degree of UPR activation and impact on proteostasis contributes to the basis of the mutation and disease severity.

Our UPR data in primary dermal fibroblasts provide direct evidence that ER stress and UPR activation are a feature of vEDS. This is supported by signs of ER stress in the vasculature, and in particular vascular fibroblasts, of a vEDS mouse model [21], defects in ER homoeostasis on transcriptomic analysis of fibroblasts [32, 33], and a delay in protein folding due to *COL3A1* glycine mutations in a bacterial expression system [34]. Thus while we employed skin fibroblasts, and we can not formally exclude some differences with vascular fibroblasts, this supports that ER stress due to glycine *COL3A1* mutations is a conserved mechanisms in fibroblasts. The detection of ER stress in fibroblasts but limited evidence from smooth muscle cells [20, 21] could reflect a cell type-dependent mechanism whereby UPR activation may occur more readily due to the higher expression of ECM proteins in fibroblasts compared to smooth muscle cells (Human Protein Atlas Dataref [35].

Recent data from mouse models explored the efficacy of modulating more downstream ERK signalling mechanisms [20]. We set out a complementary approach focusing on more upstream mechanisms that may be applicable to multiple mutations and tissues to help overcome recently observed allele

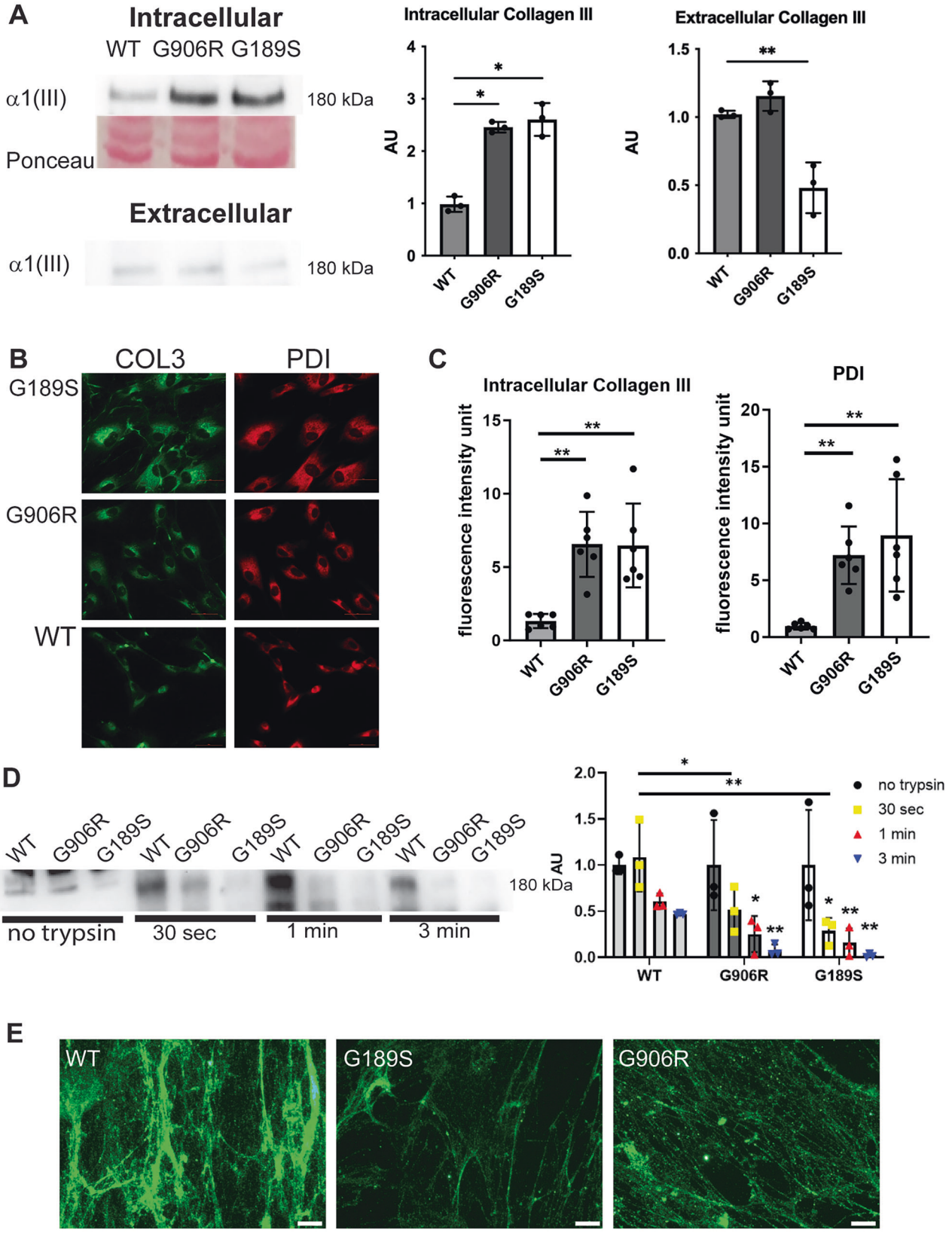

specific outcomes of treatments targeting these further downstream mechanisms [20–22]. Excitingly PBA rescued both the ER stress and improved the quality of the secreted collagen without increasing levels of secretion per se, as determined by the susceptibility to trypsin digest. This raises the intriguing prospect that PBA could rescue both cell and ECM defects. While it is necessary to extend these data into vascular cells and mouse models, the ability to ameliorate upstream molecular pathological

Fig. 2 *COL3A1* mutations affect collagen III protein handling. (**A**) Western blotting against collagen III on cellular protein lysate (intracellular) and conditioned media (extracellular) of wild type (WT), *COL3A1*$^{G189S/+}$ (G189S) and *COL3A1*$^{G906/+}$ (G906R) cells reveals intracellular retention. Ponceau total protein stain used as protein loading control. Quantification provided on right hand side. (n = 3, One Way ANOVA with Dunnett's multiple comparison test). (**B**) Immunostaining against collagen III (green) and PDI (red, ER marker) on wild type (WT), *COL3A1*$^{G189S/+}$ (G189S) and *COL3A1*$^{G906/+}$ (G906R) cells showing collagen III retention in ER in mutant cells. Size bar 50 µm. (**C**) Image J analysis using integrated density of fluorescence staining reveals ER retention and enlarged ER area (n = 6, PDI: One Way ANOVA with Dunnett's multiple comparison test, collagen III: Kruskal-Wallis test with Dunn's multiple comparison test). (**D**) Western blotting against collagen III on conditioned media that has been subjected to trypsin digestion (proxy of collagen triple helix folding) reveals secretion of mutant misfolded protein. Duration of trypsin digest is indicated. Quantification of western blot on right-hand side (n = 3, One Way ANOVA with Dunnett's multiple comparison test). (**E**) Immunostaining against collagen III (green) of decellularized matrix shows less developed collagen III ECM network and punctate appearance in mutant cells (n = 3). * p < 0.05; ** p < 0.01; *** p < 0.001.

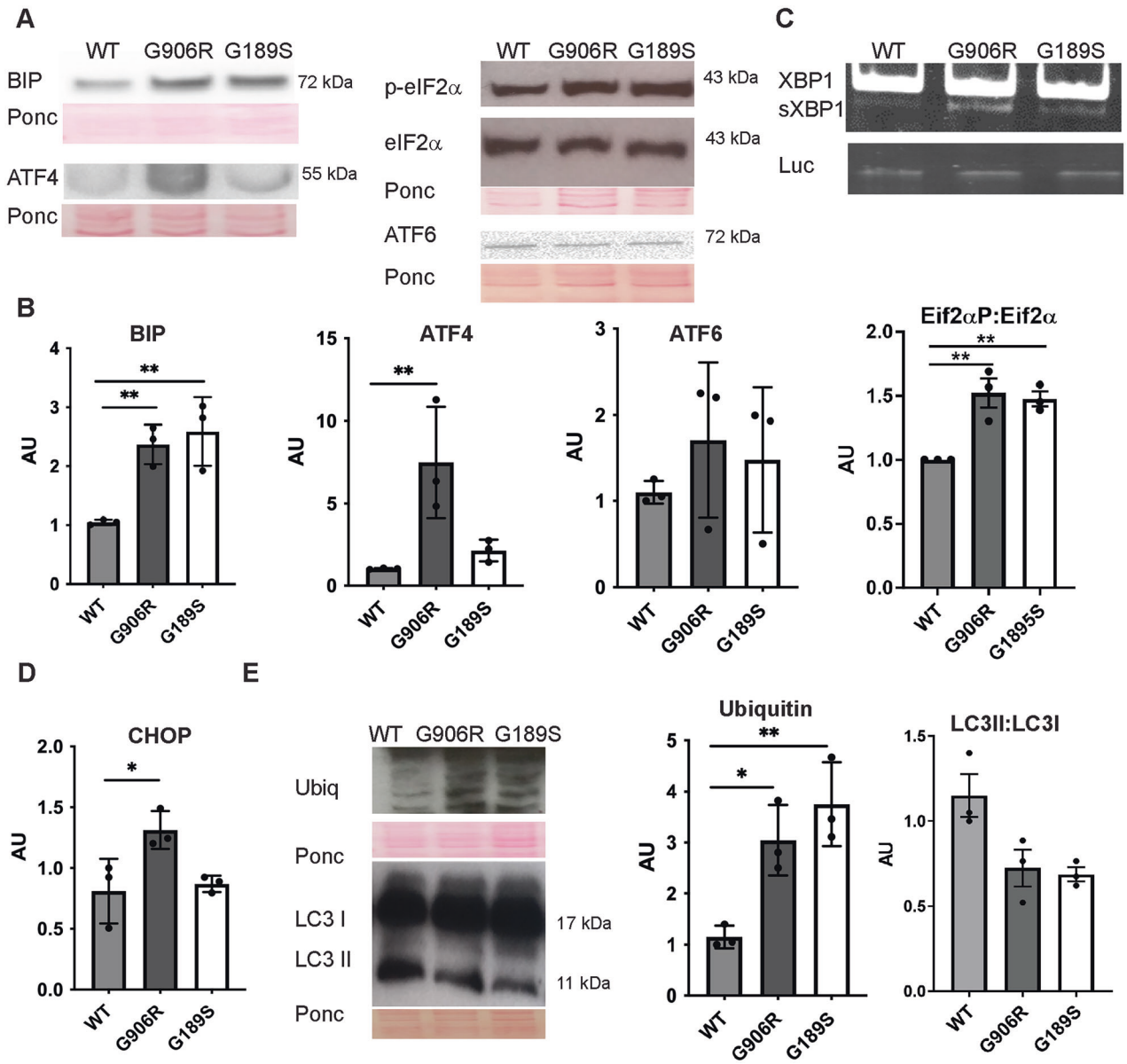

Fig. 3 *COL3A1* mutations activate ER stress. (**A**) Western blotting against ER stress markers in wild type (WT), *COL3A1*$^{G189S/+}$ (G189S) and *COL3A1*$^{G906/+}$ (G906R) cells. eIF2α: total eIF2α; p-EIF2α: phosphorylated EIF2α. Ponceau staining loading control. (**B**) Densitometry analysis of bands in (**A**) shows UPR activation in mutant cells (n = 3). (**C**) Representative gel of RT-PCR showing splicing of XBP1 by IRE1. Spliced XBP1 (sXBP1), unspliced XBP1 (XBP1), Spiked luciferase (Luc) used as loading control (see Materials and Methods for further details)(n = 3). (**D**) Measurement of CHOP mRNA levels by qRT-PCR (n = 3). (**E**) Analysis of proteasome and autophagy levels by western blotting against ubiquitinated proteins and LC3BI-II. Densitometry analysis by Image J provided in graphs on right-hand side (n = 3). B, D, E One Way ANOVA with Dunnett's multiple comparison (ATF6 Kruskal Wallis with Dunn's multiple comparisons test) * p < 0.05; ** p < 0.01.

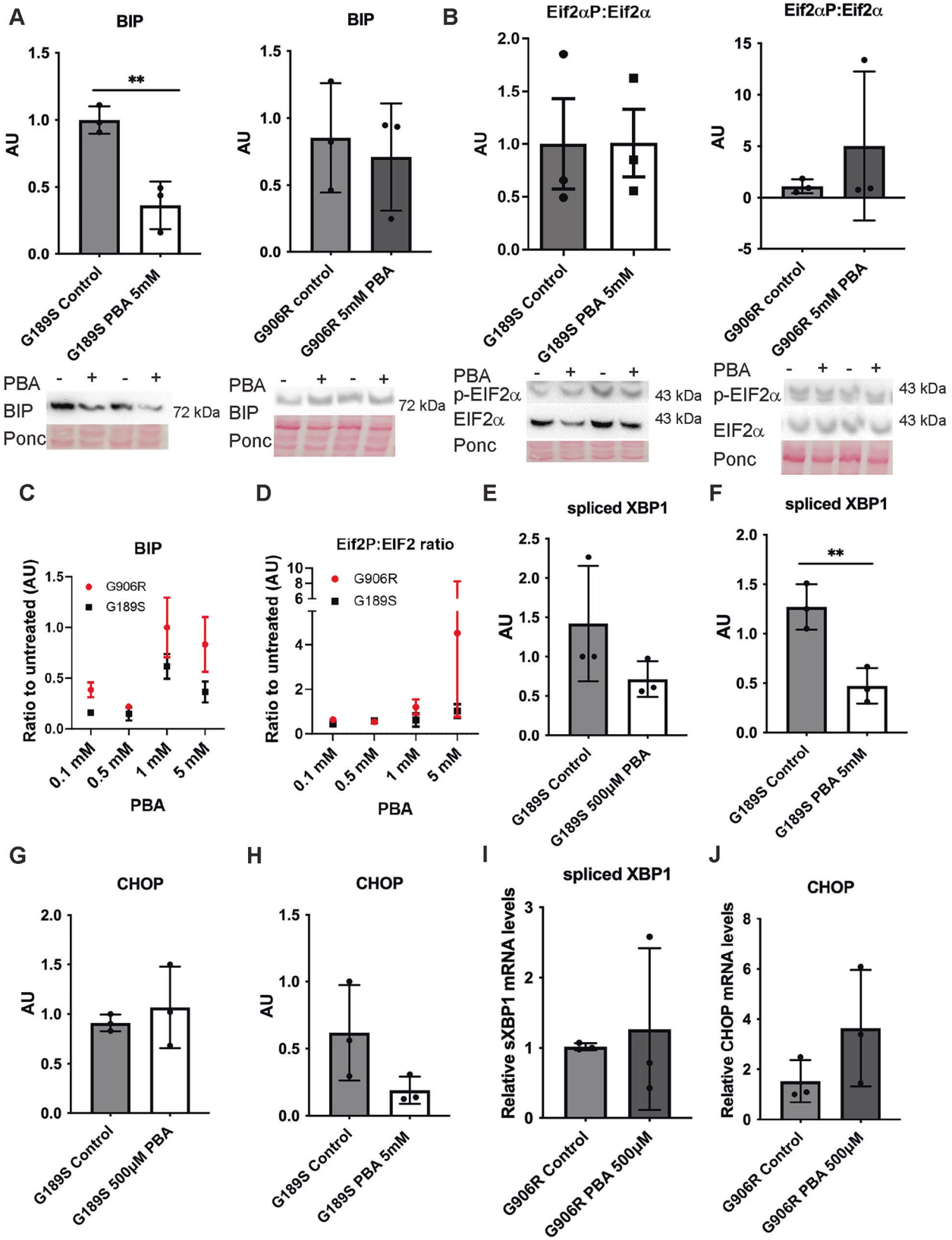

sequelae is particularly appealing for genetic disorders, such as collagenopathies and vEDS, where most patients have non re-occurring mutations [9, 36, 37]. Moreover, collagens such as collagen III are widely expressed [1] and different cell types likely have distinct downstream responses to the initial underlying pathomolecular event. Thus, the ability to modulate these initiating pathomolecular mechanisms is an attractive approach for future therapies.

Fig. 4 Efficacy of PBA in reducing intracellular defects of *COL3A1* mutations. (**A**) Western blotting against BIP in PBA-treated (PBA+ in gel) and untreated (control in graph, PBA – on gels) *COL3A1*$^{G189S/+}$ (G189S) and *COL3A1*$^{G906/+}$ (G906R) cells shows allele specific efficacy. Gels showing two biological replicates are provided below graphs of densitometry analysis using Image J (n = 3, G189S unpaired t-test, G906R Mann-Whitney test). Ponc: ponceau staining as protein loading control. (**B**) Western blotting against total (EIF2α) and phospho-eIF2α (p-EIF2α) and graphs of densitometry analysis using Image J (n = 3, G189S unpaired t-test, G906R Mann-Whitney test)). (**C**) Graph of densitometry analysis of BIP protein levels determined by western blot (gels provided in Supplemental Fig. 5) in cells incubated for 24 hours with increasing PBA concentrations (0.1 mM, 0.5 mM, 1 mM, 5 mM; n = 3). (**D**) Graph of densitometry analysis of ratio of phospho-EIF2α versus total EIF2α protein levels determined by western blot (gels provided in Supplemental Fig. 5, n = 3) in cells incubated for 24 hours with different PBA concentrations. (**E**-**F**) qRT-PCR analysis of spliced XBP1 in untreated *COL3A1*$^{G189S/+}$ cells (control) and cells treated with 500 µM and 5 mM PBA for 24 hours. (n = 3, E: Mann-Whitney test, F: unpaired t-test). (**G**-**H**) qRT-PCR analysis of CHOP in untreated *COL3A1*$^{G189S/+}$ cells (control) and cells treated with 500 µM and 5 mM PBA for 24 hours (n = 3, unpaired t-test). (**I**-**J**) qRT-PCR analysis of spliced XBP1 and CHOP in untreated *COL3A1*$^{G906R/+}$ cells (control) and treated with 500 µM for 24 hours (n = 3, unpaired t-test). * $p < 0.05$; ** $p < 0.01$.

Our data also showed that promoting protein degradation by CBZ was not able to reduce the ER stress, in contrast to *COL10A1* mutations in chondrodysplasia type Schmidt where CBZ is currently being used in a clinical trial [14]. A combination of PBA and CBZ was also not effective. Combined with data from collagen I and IV [15, 30, 38], this supports that targeting protein folding rather than degradation has more efficacy across different collagen types. This may help further stratification of collagenopathies into arms for any future mechanism-based treatments and trials targeting shared mechanisms.

In conclusion, these data establish that *COL3A1* mutations in vEDS cause ER stress via IRE1 and PERK activation, and also enable secretion of mutant protein, increasing our mechanistic insight into vEDS. Moreover, these defects were rescued by the FDA-approved chemical PBA, indicating this represents a putative therapeutic strategy that can overcome allele-specific disease mechanisms.

METHODS

Ethics approval and consent to participate

Primary fibroblast cultures were established from vEDS patients at the Centre for Medical Genetics, Ghent University Hospital, following informed consent. The research was covered by the University of Glasgow CMVLS ethics committee Ref 200200029, and experiments were performed in accordance with local guidelines and regulations.

Cell culture and drug treatments

Primary fibroblast cultures were established from vEDS patients and controls are ethnically matched commercially available primary dermal fibroblasts (TCS Cell Works and Lonza (UK)). Cells were maintained in DMEM, 10% (control cells) or 15% FBS (*COL3A1* mutant cells) and 1% penicillin/streptomycin in 37 °C. This higher % FBS increases proliferation and ease of culturing fibroblasts carrying collagen mutations. For experiments cells (passage number 8-12) were cultured in DMEM containing 10% FBS, 1% penicillin/streptomycin and 0.25 mM ascorbic acid for 72 hours to promote collagen expression and folding [39]. Cells were incubated with 4-PBA (PCI synthesis), tauroursodeoxycholic acid (TUDCA, Merck), carbamazepine (CBZ, Merck)) or Bafilomycin A1 (Cell Signalling) for the last 24 or 72 hours. To assess cell proliferation 30,000 cells were plated and counted using a haemocytometer.

Western blotting

Protein extracts were prepared in RIPA buffer containing protease (Complete Mini, Roche) and phosphatase (PhosSTOP, Roche) inhibitors. For western blotting on conditioned media, cells were cultured for final 24 hours in under serum-free conditions and 20 µl of conditioned media was used. Protein samples were prepared and denatured in Laemmli Buffer and SDS-PAGE was performed under reducing conditions (Mini-PROTEAN® Tetra, Bio-Rad) before transfer onto membranes. Following blocking (5% milk/BSA) membranes were incubated with primary antibody overnight at 4 °C (BIP [1:40,000 BD Transduction 610979], ATF4 [1:1000, Santa Cruz Biotechnology sc-200], ATF6 [1:1000 Abcam ab122897], Collagen III [1:1000, Abcam ab7778], Phospho-eIF2α (Ser51) [1:1000, Cell Signalling Technology 9721], eIF2α [1:1000, Cell Signalling Technology 9722], ubiquitin [1:1000, Santa Cruz Biotechnology P491], LC3B [1:500, Novus Biologicals 1251 A], Tubulin [1:40,000 Sigma T5168], p62 [1:1000, Proteinech 18420-1-AP]). Following HRP-conjugated secondary antibody incubation (1:1000, Cell Signalling Technology), membranes were incubated with Luminata Forte Western HRP substrate (Millipore) before visualization using a BioRad ChemicDoc XRS+ or X-OMAT- Film processor using Hyperfilm™ ECL (GE Healthcare).

Trypsin digestion of collagen

Cells were cultured for final 24 hours in under serum-free conditions. 30 µl conditioned medium from cells was treated with 1 µl 0.05% trypsin at 46 °C for 30 s, 1 min or 3 min. Trypsin was inactivated by adding 1 µl 0.1% trypsin inhibitor (Sigma) and denaturation at 95 °C for 5 min. Samples were analyzed using western blot.

qRT-PCR

Cells were incubated with Trizol (ThermoFisher) and RNA was extracted and resuspended in nuclease free water as per manufacturer's Instruction, and purity and concentration determined using a nanodrop ND1000 spectrophotometer (Thermo Scientific). RNA samples were treated with DNA-free™ DNA Removal Kit (ThermoFisher) as per manufacturer's Instruction, and subsequently spiked with luciferase (50 pg/µg RNA). Following cDNA synthesis (High Capacity cDNA Reverse Transcription Kit (Thermofisher), qRT-PCR was performed using Power Up SYBR green Master mix (Invitrogen; 7900HT Fast Real-Time PCR Applied Biosystems). Samples were normalized to 18S RNA and/or luciferase and relative mRNA levels were calculated using the $2^{-\Delta\Delta CT}$ method. Primer sequences: CHOP (GCGCATGAAGGAGAAAGAAC, TCTGGGAAAGGTGGGTAGTG), IRE1 (CGGGAGAACATCACTGTCCC, CCCGGTAGTGGTGCTTCTTA), COL3A1 (TGGTCTGCAAGGAATGCCTGGA, TCTTTCCCTGGGACACCATCAG), 18S (AGTCCCTGCCCTTTGTACACA, CGATCCGAGGGCCTCACTA), luciferase (GCTGGGCGTTAATCAGAGAG, GTGTTCGTGTTCGTCCCAGT).

Analysis of apoptosis

Apoptosis was measured using FITC Annexin V Apoptosis Detection Kit I (BD biosciences). 1×10^5 cells were stained and cells (6000 events/sample) were analysed in triplicate using a BD FACS Canto II and FlowJo Software. Unstained, FITC stained only, PI stained only and positive control (DMSO-induced apoptosis) cells were used to calibrate the machine.

MTT cell viability assay

Cells were seeded at a density of 5×10^3 cells in 100 µl culture media in triplicates and cultured for 72 h with 0.25 mM ascorbic acid and 10 nM bafilomycin A1. Following treatment, cell viability was then measured using the CyQuant MTT cell viability assay kit (V13154, Invitrogen) as per manufacturer's instructions. MTT reagent was added to cells for 4 h at 37 °C in 5% CO2 humidified incubator. MTT added to medium only served as the negative control. After incubation, DMSO was added in each well and cells were incubated for an additional 10 min. Absorbance was then measured at 540 nm wavelength on a microplate spectrophotometer (MultiSkan SkyHigh, Thermo Scientific).

Immunohistochemistry

Staining was performed as described [16]. Cells were fixed (acetone, 10% methanol, or 4% PFA), and incubated with 0.05 M KCL/0.05 M HCL for antigen retrieval. Following blocking, cells were incubated with primary antibodies in 10% goat serum 4 °C overnight (collagen III [1:300, Abcam ab778], PDI [P4HB 1:200, Abcam ab2792]. Cells were washed, incubated

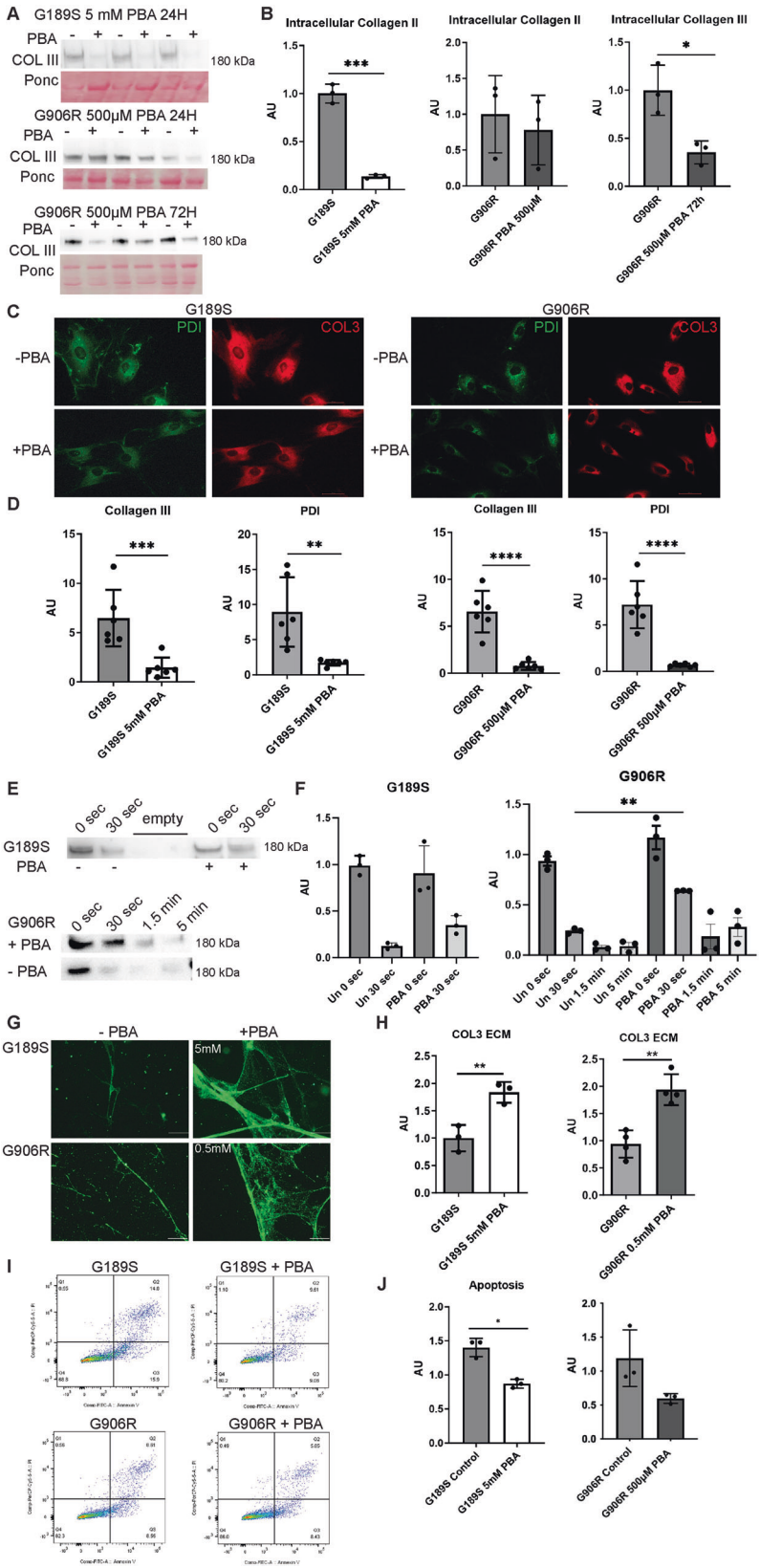

with secondary antibody (Cy2, Cy3 conjugated, 1:500 Jackson Immunoresearch) in 1% goat serum. Following washes, cells were incubated with DAPI, washed, and mounted prior to imaging on a Nikon eclipse Tg2 fluorescence microscope.

For extracellular collagen III staining cells were seeded on coverslips, cultured for 24 h prior to 72 h culturing in media containing 0.25 mM ascorbic acid with/without PBA. Coverslips were washed prior to decellularization by incubating with 20 mM NH_4OH (30 min at RT) followed

Fig. 5 PBA dosage and rescue of cell and ECM defects. (**A**) Western blotting against intracellular collagen III on untreated (-) and PBA-treated cells (+). *COL3A1*$^{G906R/+}$ cells were treated with 500 µM PBA for 24 and 72 hours. (**B**) Densitometry analysis of gels in (A) (n = 3). (**C**) Immunostaining against collagen III (red) and PDI (green, ER marker) on untreated (-PBA) and PBA treated (+ PBA) *COL3A1*$^{G189S/+}$ (G189S) and *COL3A1*$^{G906/+}$ (G906R) cells. *COL3A1*$^{G189S/+}$ (G189S) was treated with 5 mM PBA for 24 hours, *COL3A1*$^{G906/+}$ with 500 M PBA for 72 hours. Scale bar 50 µm. (**D**) Image J analysis using integrated density of fluorescence staining reveals reduced ER retention of collagen III and ER area in PBA treated cells (n = 6). (**E**) Western blotting against collagen III on conditioned media from untreated (PBA -) and PBA (PBA +) treated cells that has been subjected to trypsin digestion. *COL3A1*$^{G189S/+}$ (G189S) was treated with 5 mM PBA for 24 hours, *COL3A1*$^{G906/+}$ with 500 M PBA for 72 hours. Duration of trypsin digest is indicated. (**F**) Quantification of western blot on right-hand side supports PBA increased resistance to trypsin digest (n = 3). (**G**) Immunostaining against collagen III (green) on decellularized deposited ECM from untreated and PBA treated cells. *COL3A1*$^{G189S/+}$ (G189S) and *COL3A1*$^{G906/+}$ (G906R) cells were incubated three days with 5 mM and 500 µM PBA respectively. Scale bar 10 µm. (**H**) Integrated density of collagen III staining shown in (G)(n = 3). (**I**) FACS scatter plot of untreated (G189S, G906R) and treated cells (+ PBA) stained with propidium iodide (PI) and Annexin V. *COL3A1*$^{G189S/+}$ (G189S) was treated with 5 mM PBA for 24 hours, *COL3A1*$^{G906/+}$ with 500 M PBA for 72 hours. (**J**) Graphs of apoptosis levels as determined by FACS in (I) showed PBA reduced apoptosis.

by washes. The matrix was fixed with 4% PFA (10 min, RT), washed, blocked in 10% goat serum in PBS (1 h RT), and washed thrice. Samples were incubated with anti-collagen III antibody (1:100, Abcam ab7778) overnight at 4 °C. Following washes, samples were incubated with secondary antibody (1:300, goat-anti-rabbit Alexa Fluor 488, ab150077, RT, 1 hour), mounted and imaged using a Nikon Eclipse Ts2 microscope using NIS Elements Software (Nikon). Matrix deposition was quantified by measuring integrated density (Image J). Values were averaged across 5 images/coverslip per n number. Co-localisation coefficients (Pearson's R) were calculated using the JaCop (Just another Colocalization plugin) in Image J [40]. Fishers z-transformation was then applied to convert individual R values to Fisher's z, these were then averaged and converted back to obtain the average Pearson's R.

EM analysis

Cell pellets were fixed in 2% (v/v) formaldehyde and 2.5% (v/v) glutaraldehyde in 100 mM cacodylate buffer, pH 7.4, at 4 °C overnight. After washing in PBS, samples were postfixed in 0.5% (v/v) osmium tetroxide and 1% (w/v) potassium hexacyanoferrate (III) in 0.1 M cacodylate buffer for 2 h at 4 °C followed by washing with distilled water. After dehydration in an ascending ethanol series from 30 to 100% ethanol, specimens were two times incubated in propylene oxide each for 15 min and embedded in Epon using flat embedding molds. Ultrathin sections were cut with an ultramicrotome, collected on copper grids and negatively stained with 2% uranyl acetate for 10 min. Electron micrographs were taken at 60 kV with a Veleta camera system in combination with the Radius software system (emsis, Münster, Germany).

Statistical analysis

Statistical analysis was performed using the GraphPad Prism software. Unpaired Student t-test, One-Way ANOVA with post hoc correction, or 2-way ANOVA were used as appropriate following normality testing (Shapiro Wilk test). In case of non normal data distribution Mann-Whitney or Kruskal Wallis (with Dunn's multiple comparisons test) was used. Sample size based on previous experience. Calculation performed under equal variance. p-value < 0.05 was considered statistically significant. * $p < 0.05$; ** $p < 0.01$; *** $p < 0.001$.

DATA AVAILABILITY

The datasets generated during and/or analysed during the current study are available from the corresponding author on reasonable request.

REFERENCES

1. Omar R, Malfait F, Van Agtmael T. Four decades in the making: Collagen III and mechanisms of vascular Ehlers Danlos Syndrome. Matrix Biol. 2021;12:100090 https://doi.org/10.1016/j.mbplus.2021.100090.
2. Pepin M, Schwarze U, Superti-Furga A, Byers PH. Clinical and genetic features of ehlers–danlos syndrome type IV, the Vascular Type. N Engl J Med. 2000;342:673–80. https://doi.org/10.1056/nejm200003093421001.
3. Byers PH, Belmont J, Black J, De Backer J, Frank M, Jeunemaitre X, et al. Diagnosis, natural history, and management in vascular Ehlers–Danlos syndrome. Am J Med Genet Part C: Semin Med Genet. 2017;175:40–7. https://doi.org/10.1002/ajmg.c.31553.
4. Fagerberg L, Hallström BM, Oksvold P, Kampf C, Djureinovic D, Odeberg J, et al. Analysis of the human tissue-specific expression by genome-wide integration of transcriptomics and antibody-based proteomics. Mol Cell Proteom. 2014;13:397–406. https://doi.org/10.1074/mcp.M113.035600.
5. Yue F, Cheng Y, Breschi A, Vierstra J, Wu W, Ryba T, et al. A comparative encyclopedia of DNA elements in the mouse genome. Nature. 2014;515:355–64. https://doi.org/10.1038/nature13992.
6. Kuivaniemi H, Tromp G. Type III collagen (COL3A1): Gene and protein structure, tissue distribution, and associated diseases. Gene. 2019;707:151–71. https://doi.org/10.1016/j.gene.2019.05.003.
7. BÄCHINGER HP, BRUCKNER P, TIMPL R, PROCKOP DJ, ENGEL J. Folding Mechanism of the Triple Helix in Type-III Collagen and Type-III pN–Collagen. Eur J Biochem. 1980;106:619–32. https://doi.org/10.1111/j.1432-1033.1980.tb04610.x.
8. Bächinger HP, Fessler LI, Timpl R, Fessler JH. Chain assembly intermediate in the biosynthesis of type III procollagen in chick embryo blood vessels. J Biol Chem. 1981;256:13193–9. https://doi.org/10.1016/S0021-9258(18)43026-8.
9. Pepin MG, Schwarze U, Rice KM, Liu M, Leistritz D, Byers PH. Survival is affected by mutation type and molecular mechanism in vascular Ehlers–Danlos syndrome (EDS type IV). Genet Med. 2014;16:881–8. https://doi.org/10.1038/gim.2014.72.
10. Frank M, Albuisson J, Ranque B, Golmard L, Mazzella J-M, Bal-Theoleyre L, et al. The type of variants at the COL3A1 gene associates with the phenotype and severity of vascular Ehlers–Danlos syndrome. Eur J Hum Genet. 2015;23:1657–64. https://doi.org/10.1038/ejhg.2015.32.
11. Pieri M, Stefanou C, Zaravinos A, Erguler K, Stylianou K, Lapathitis G, et al. Evidence for activation of the unfolded protein response in collagen IV nephropathies. J Am Soc Nephrol. 2014;25:260–75. https://doi.org/10.1681/asn.2012121217.
12. Jones FE, Bailey MA, Murray LS, Lu Y, McNeilly S, Schlotzer-Schrehardt U, et al. ER stress and basement membrane defects combine to cause glomerular and tubular renal disease resulting from Col4a1 mutations in mice. Dis Model Mech. 2016;9:165–76. https://doi.org/10.1242/dmm.021741.
13. Gioia R, Tonelli F, Ceppi I, Biggiogera M, Leikin S, Fisher S, et al. The chaperone activity of 4PBA ameliorates the skeletal phenotype of Chihuahua, a zebrafish model for dominant osteogenesis imperfecta. Hum Mol Genet. 2017;26:2897–911. https://doi.org/10.1093/hmg/ddx171.
14. Mullan LA, Mularczyk EJ, Kung LH, Forouhan M, Wragg JMA, Goodacre R, et al. Increased intracellular proteolysis reduces disease severity in an ER stress–associated dwarfism. J Clin Invest. 2017;127:3861–5. https://doi.org/10.1172/JCI93094.
15. Jones FE, Murray LS, McNeilly S, Dean A, Aman A, Lu Y, et al. 4-Sodium phenyl butyric acid has both efficacy and counter-indicative effects in the treatment of Col4a1 disease. Hum Mol Genet. 2019;28:628–38. https://doi.org/10.1093/hmg/ddy369.
16. Murray LS, Lu Y, Taggart A, Van Regemorter N, Vilain C, Abramowicz M, et al. Chemical chaperone treatment reduces intracellular accumulation of mutant collagen IV and ameliorates the cellular phenotype of a COL4A2 mutation that causes haemorrhagic stroke. Hum Mol Genet. 2014;23:283–92. https://doi.org/10.1093/hmg/ddt418.
17. Wang D, Mohammad M, Wang Y, Tan R, Murray LS, Ricardo S, et al. The chemical chaperone, PBA, reduces ER stress and autophagy and increases collagen IV α5 expression in cultured fibroblasts from men with X-linked alport syndrome and missense mutations. Kidney Int Rep. 2017;2:739–48. https://doi.org/10.1016/j.ekir.2017.03.004.
18. Frank M, Adham S, Seigle S, Legrand A, Mirault T, Henneton P, et al. Vascular Ehlers-Danlos Syndrome: Long-Term Observational Study. J Am Coll Cardiol. 2019;73:1948–57. https://doi.org/10.1016/j.jacc.2019.01.058.
19. Baderkhan H, Stenborg A, Hägg A, Wanhainen A, Björck M. Celiprolol Treatment of Patients With Vascular Ehlers-Danlos Syndrome. Eur J Vasc Endovasc Surg. 2019;58:e627 https://doi.org/10.1016/j.ejvs.2019.09.115.
20. Bowen CJ, Calderón Giadrosic JF, Burger Z, Rykiel G, Davis EC, Helmers MR, et al. Targetable cellular signaling events mediate vascular pathology in vascular Ehlers-Danlos syndrome. J Clin Invest. 2020;130:686–98. https://doi.org/10.1172/JCI130730.

21. Legrand A, Guery C, Faugeroux J, Fontaine E, Beugnon C, Gianfermi A, et al. Comparative therapeutic strategies for preventing aortic rupture in a mouse model of vascular Ehlers-Danlos syndrome. PLoS Genet. 2022;18:e1010059 https://doi.org/10.1371/journal.pgen.1010059.
22. Dubacher N, Münger J, Gorosabel MC, Crabb J, Ksiazek AA, Caspar SM, et al. Celiprolol but not losartan improves the biomechanical integrity of the aorta in a mouse model of vascular Ehlers–Danlos syndrome. Cardiovasc Res. 2019;116:457–65. https://doi.org/10.1093/cvr/cvz095.
23. Zhao H, Darzynkiewicz Z. Biomarkers of cell senescence assessed by imaging cytometry. Methods Mol Biol. 2013;965:83–92. https://doi.org/10.1007/978-1-62703-239-1_5.
24. Shtutman M, Chang BD, Schools GP, Broude EV. Cellular Model of p21-Induced Senescence. Methods Mol Biol. 2017;1534:31–9. https://doi.org/10.1007/978-1-4939-6670-7_3.
25. Gatseva A, Sin Yuan Y, Brezzo G, Van Agtmael T. Basement membrane collagens and disease mechanisms. Essays Biochem. 2019;63:297–312. https://doi.org/10.1042/ebc20180071.
26. Lamandé SR, Bateman JF Genetic Disorders of the Extracellular Matrix. The Anatomical Record. 2019;0. https://doi.org/10.1002/ar.24086.
27. Jeanne M, Jorgensen J, Gould DB. Molecular and Genetic Analysis of Collagen Type IV Mutant Mouse Models of Spontaneous Intracerebral Hemorrhage Identify Mechanisms for Stroke Prevention. Circulation. 2015;131:1555–65. https://doi.org/10.1161/circulationaha.114.013395.
28. Engin F, Hotamisligil GS. Restoring endoplasmic reticulum function by chemical chaperones: an emerging therapeutic approach for metabolic diseases. Diabetes Obes Metab. 2010;12:108–15.
29. Jonker AH, O'Connor D, Cavaller-Bellaubi M, Fetro C, Gogou M, 'T Hoen PAC, et al. Drug repurposing for rare: progress and opportunities for the rare disease community. Frontiers in Medicine. 2024;11. https://doi.org/10.3389/fmed.2024.1352803.
30. Garibaldi N, Contento BM, Babini G, Morini J, Siciliani S, Biggiogera M, et al. Targeting cellular stress in vitro improves osteoblast homeostasis, matrix collagen content and mineralization in two murine models of osteogenesis imperfecta. Matrix Biol. https://doi.org/10.1016/j.matbio.2021.03.001 2021.
31. Marini JC, Forlino A, Cabral WA, Barnes AM, San Antonio JD, Milgrom S, et al. Consortium for osteogenesis imperfecta mutations in the helical domain of type I collagen: regions rich in lethal mutations align with collagen binding sites for integrins and proteoglycans. Hum Mutat. 2007;28:209–21. https://doi.org/10.1002/humu.20429.
32. Chiarelli N, Carini G, Zoppi N, Ritelli M, Colombi M. Transcriptome analysis of skin fibroblasts with dominant negative COL3A1 mutations provides molecular insights into the etiopathology of vascular Ehlers-Danlos syndrome. PLoS One. 2018;13:e0191220 https://doi.org/10.1371/journal.pone.0191220.
33. Chiarelli N, Ritelli M, Zoppi N, Colombi M. Cellular and Molecular Mechanisms in the Pathogenesis of Classical, Vascular, and Hypermobile Ehlers–Danlos Syndromes. Genes. 2019;10:609.
34. Mizuno K, Boudko S, Engel J, Bächinger HP. Vascular Ehlers-Danlos Syndrome Mutations in Type III Collagen Differently Stall the Triple Helical Folding *. J Biol Chem. 2013;288:19166–76. https://doi.org/10.1074/jbc.M113.462002.
35. Karlsson M, Zhang C, Méar L, Zhong W, Digre A, Katona B, et al. A single–cell type transcriptomics map of human tissues. Science Adv. 2021;7:eabh2169 https://doi.org/10.1126/sciadv.abh2169.
36. Malfait F, Castori M, Francomano CA, Giunta C, Kosho T, Byers PH. The Ehlers–Danlos syndromes. Nature Rev Dis Prim. 2020;6:64 https://doi.org/10.1038/s41572-020-0194-9.
37. Jeanne M, Gould DB. Genotype-phenotype correlations in pathology caused by collagen type IV alpha 1 and 2 mutations. Matrix Biol. 2017;57-58:29–44. https://doi.org/10.1016/j.matbio.2016.10.003.
38. Dean A, Van Agtmael T Collagen IV-Related Diseases and Therapies. In: Ruggiero F, editor. The Collagen Superfamily and Collagenopathies. Cham: Springer International Publishing; 2021. p. 143-97.
39. Geesin JC, Darr D, Kaufman R, Murad S, Pinnell SR. Ascorbic acid specifically increases type I and type III procollagen messenger RNA levels in human skin fibroblast. J Invest Dermatol. 1988;90:420–4. https://doi.org/10.1111/1523-1747.ep12460849.
40. Manders EMM, Verbeek FJ, Aten JA. Measurement of co-localization of objects in dual-colour confocal images. J Microsc. 1993;169:375–82. https://doi.org/10.1111/j.1365-2818.1993.tb03313.x.

ACKNOWLEDGEMENTS

We would like to thank the patients and their families for their participation in this project. This work was funded by the University of Glasgow MVLS DTP scholarship to RO; BHF to LGT (FS/4yPhD/F/20/34127); MRC Project (MR/R005567/1), Stroke Association (16VAD_04), EPSRC (EP/X031721/1; Horizon Europe MSCA Doctoral Network 101072766 CHANGE) and Heart Research UK Translational (RG 2664/17/20) awards to TVA. FM is a senior clinical investigator of the Research Foundation Flanders (1842318 N), and this work funded by Ghent University (GOA019-21).

AUTHOR CONTRIBUTIONS

Study design and concept: RO, NJB, FM & TVA; Experimental work RO, MAWL, LGT, SH, MAA, UH, CRT, OMEHEA, TVA, SL, JC (supervised by AMM); Data Analysis: RO, MAWL, LGT, CRT, UH, FM, TVA; Writing of the manuscript: all authors. NJB co-designed the project and co-supervised RO together with TVA, but sadly passed away 22 March 2023.

COMPETING INTERESTS

The authors declare no competing of interests.

ADDITIONAL INFORMATION

Supplementary information The online version contains supplementary material available at https://doi.org/10.1038/s41420-025-02476-y.

Correspondence and requests for materials should be addressed to Tom Van Agtmael.